Implantation-induced structural changes in evaporated amorphous Ge

Gábor Petö and Zsolt F. Horváth
Research Institute for Materials Science, Budapest, P.O. Box 49, H-1525, Hungary

Orsolya Gereben and László Pusztai
Laboratory of Theoretical Chemistry, Lóránd Eötvös University, Budapest 112, P.O. Box 32, H-1518, Hungary

Ferenc Hajdú and Erzsébet Sváb
Research Institute for Solid State Physics, Budapest, P.O. Box 49, H-1525, Hungary
(Received 3 February 1994)

The short-range structure of amorphous germanium in the as-evaporated state and after Sb-ion implantation was investigated by x-ray diffraction. Significant changes were detected in the structure factors of the two specimens. Reverse Monte Carlo analyses of both data were carried out. An increase of 12–15% in the atomic number density due to implantation was established. The diffraction data are consistent both with an atomic arrangement where the originally defective structure becomes nearly perfect as a consequense of the ion bombardment, or with the formation of a new phase of *a*-Ge with an average first coordination number higher than 4.

The structural properties of amorphous Si and Ge have been investigated extensively.[1–7] It was demonstrated in the early 1970s that the first neighbors are tetrahedrally coordinated and the structural parameters such as bond angles, bond lengths, and first and second shell coordination numbers are very similar to those of crystalline Ge or Si. This structural similarity corresponds to the similar physical properties of *a*-Ge vs *c*-Ge or *a*-Si vs *c*-Si.

Many experimental efforts have been made to prepare different amorphous samples from Si and Ge. However, their structural and physical properties were very similar in most cases. It is widely accepted that any difference in the experimentally observed parameters, i.e., somewhat different values of the coordination numbers, can be regarded as the properties of the actual sample and not as a basic difference in the structure of *a*-Si or *a*-Ge.

Ion implantation is not a very common, but useful tool for the formation of *a*-Si or *a*-Ge. Structural characteristics of implanted samples have not been studied so far. On the other hand, differences were found[8] between the photoemission spectra of evaporated and ion-implanted *a*-Si. Moreover, the measured valence band density of states in *a*-Ge induced by ion implantation showed that the rehybridization of the sp^3 state is possible, causing deviation from the tetrahedral local order.

In order to clarify the structural background of the detected modifications in the valence energy band, an x-ray diffraction study has been performed on *a*-Ge, both in as-evaporated and in Sb-ion-implanted states. Reverse Monte Carlo (RMC) simulation,[9] a method for structural modeling and/or diffraction data analysis of noncrystalline materials, was used for revealing the differences between the two (evaporated and implanted) states.

Sample preparation is a crucial point of this work as the available mass of the implanted material is less than that usually required for an x-ray diffraction study. This is because of the limited thickness of the layer that can be treated in its full depth by ion implantation. The problem was solved by producing a multilayer system of seven layers, where the amorphous germanium films were evaporated and after that implanted, successively, under the same conditions. The thickness of a single layer and the parameters of implantation were optimized in a way to meet two opposite demands, namely, to prepare homogeneously implanted material in the whole depth, and to avoid interaction (ion induced annealing) between the sequential implanted layers.

The evaporation was done under 5×10^{-5} Pa pressure on an Al substrate (99.99%) covered by photoresist lacquer (AZ-1300) of less than 0.5 μm thickness. The substrate was kept at room temperature, and no anealing was performed. The thickness of the single germanium layer was about 800–1000 Å. Each layer was implanted by $^{121}Sb^+$ of 80 keV energy, of 10^{15} ions/cm^2 dose, and 1 μA/cm^2 current density. The number of Sb ions implanted into the material is estimated to be about 0.5 at.% of Ge atoms.

The lacquer layer enabled the multilayer set up to be easily removed from the substrate, without any contamination of the Al sheet. The material mounted on a Si(111) substrate was checked by transmission electron microscopy (TEM). Figure 1 shows this multilayer structure where the seven layers are clearly separated. It can be seen that the lower part of each layer, to about half of the whole depth, is damaged heavily due to implantation. In this region relatively large cavities (bright areas) have been formed, whereas smaller spots can be observed deeper. It is supposed that the damaged material (dark region) has become more dense due to ion bombardment. The morphology is characterized by columns of *a*-Ge of about 100–200 Å length and 30–40 Å diameter. As was shown earlier,[10] the ultraviolet photoemission spectroscopy (UPS) spectrum changes gradually as a function of the depth. This finding suggests that there

FIG. 1. TEM micrograph of the ion-implanted sample.

are changes in the short-range interactions when moving from the surface towards the bulk of the implanted material. It is supposed that these changes would be reflected by the microscopic structure of the sample, to be studied by x-ray diffraction.

X-ray diffraction measurements have been performed on a PC-controlled powder diffractometer using monochromated Mo $K\alpha$ radiation in transmission arrangement covering the momentum transfer range of Q= 0.1–14 Å^{-1}. Technical details of the measurement and data treatment have been described earlier.[11] The thickness of the Ge thin films had to be kept very low because of ion implantation—as was described above—and so both samples were far from being of optimum thickness for Mo $K\alpha$ radiation, claiming a very careful data treatment. The scattering of the sample holder thin plastic foil was precisely subtracted, but its use has certainly increased the statistical fluctuations of measured intensities, and thus real structural oscillations above 10 Å^{-1} were not available. Systematic errors could stem from these nonideal circumstances. However, as all conditions of the measurements were identical, and here mainly the *differences* between the samples are concerned, effects of systematic errors, assumed to be identical for the two measurements, cancel out.

Figure 2 shows the structure factors, $S(Q)$, obtained for the evaporated and implanted a-Ge samples. It is evident that there are slight but significant differences between the two spectra, especially around the second and third peaks. The intensities of these peaks are higher by about 10% for the implanted sample and there is a slight shift towards higher Q values. It is remarkable that the intensities of the first peaks—both at 1.9 Å^{-1}—do not show any differences. The $S(Q)$ of the evaporated

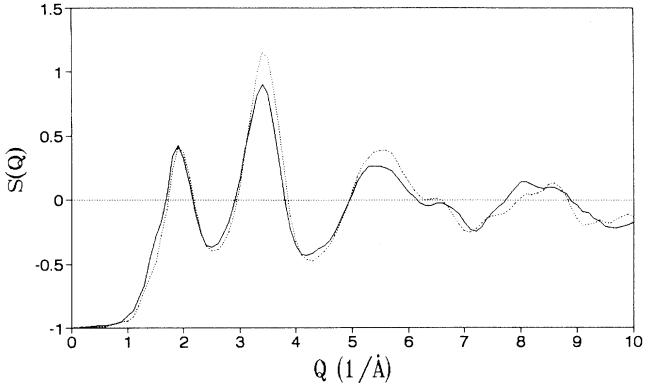

FIG. 2. Measured structure factor of evaporated (solid) and ion-implanted (dashed) amorphous Ge.

a-Ge sample is in good agreement with earlier x-ray[1] and neutron[2] diffraction results. This fact also gives support for neglecting effects of systematic errors.

The average number density, ϱ_0, was adjusted so that the radial distribution function oscillates about zero before the first true peak and takes a positive value immediately after it. A similar method was used in Refs. 2 and 12. As a result of this procedure we found ϱ_{ev}=0.040 ± 0.003 Å^{-3} and ϱ_{im}=0.046 ± 0.003 Å^{-3}. Using these values first neighbor coordination numbers of 3.6 ± 0.2 and 4.1 ± 0.2 were obtained for the evaporated and ion-implanted specimens, respectively. This means that a significant density increase of about 15% takes place as a consequence of implantation. Note that ϱ_{ev} is less than the density of c-Ge, ϱ_{cr}=0.0442 Å^{-3}, by 10%, and it is in full agreement with the result published in Ref. 2. On the other hand, ϱ_{im} is above ϱ_{cr} by 5%, which agrees with the density of liquid germanium, measured at 980°C by x-ray diffraction.[12]

The microscopic density is a fundamental quantity in this study, since using incorrect values of it leads to false coordination numbers. This is why another route for determining ϱ_0, and particularly the *change* of it upon implantation, was facilitated. RMC simulation has recently been shown to be able to guess the correct number density if the structure factor is used for modeling.[13] In the current study a systematic RMC survey has been performed to get the correct density values. A summary of these calculations is given in Fig. 3, where well-defined minima can be found in the least squares difference curves, as functions of the number density. The best fits are obtained when ϱ_{ev}=0.0375 ± 0.002 Å^{-3} and ϱ_{im}=0.042 ± 0.002 Å^{-3}, and the corresponding average first neighbor coordination numbers are n_{ev}=3.3 ± 0.2 and n_{im}=3.95 ± 0.2 for the evaporated and implanted states, respectively. The difference of at least 12% clearly separates the two states. Note that the density values calculated using the traditional way are somewhat higher for both samples. This can be explained by taking into account the argument of Cargill.[14] According to that, traditional evaluation of diffraction data that were taken on samples with considerable density variation (e.g, on those containing voids) always leads to number densities that are higher than the real density of scattering centres, if the effect of very small angle scattering is ne-

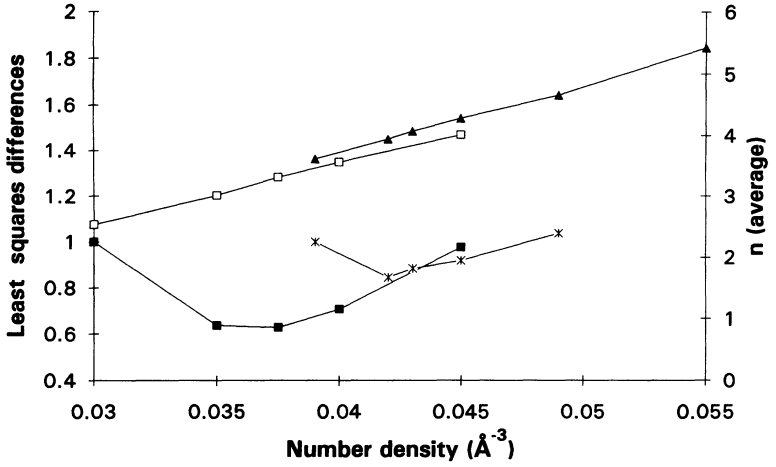

FIG. 3. Least squares differences vs number density curves for evaporated (solid squares) and ion-implanted (asterisks) amorphous Ge. Average first coordination numbers are also given: evaporated, open squares, implanted, solid triangles.

glected. However, it is encouraging that both methods provide consistently the same density difference between the two states.

In all simulations (including those for the density search) a cubic system of $N = 1728$ particles was used. A hard core diameter of 1.9 Å helped to avoid physically meaningless configurations. The system size enabled us to carry out the calculations in Q space, using the experimentally determined structure factors in the Q range of 0–10 Å^{-1}. The starting configuration was always a perfect diamond lattice. For the evaporated case 7×10^5, whereas for the implanted case 5.3×10^5 accepted moves were completed. The fits to the experimental data sets can be seen in Fig. 4. The most important fact is that the differences between the two data sets are significantly larger than the deviations between corresponding experimental and RMC calculated structure factors. This forms the basis of further discussions.

Pair correlation functions, $g(r)$, of the evaporated and implanted states are given in Fig. 5. These $g(r)$ functions are directly calculated from the atomic positions in the simulation boxes. There are distinct differences between the two $g(r)$, especially around and beyond the second peak. It is difficult to tell exactly the origin of this deviation, although on the basis of previous studies[4] on amorphous Si it is suggested that the implanted structure is closer to a tetrahedral network (see also below).

Figure 6 compares distributions of the number of first neighbors for the two samples. The average values of the first coordination number were evaluated on the basis of these distributions. Clearly, the distribution corresponding to the implanted state is centered around $m = 4$, whereas the other curve peaks at $m = 3$. Note that the difference between the two distributions is slightly larger than it could be expected solely on the basis of density differences. The broad distributions are probably not real for any of the samples, and they could have been made narrower by imposing constraints (see Ref. 4). However, doing so would have affected an unbiased comparison.

Figure 7 provides the comparison of cosine distributions of bond angles. The differences might seem minor, but they are in fact highly consequential. Shifting towards the implanted state, the peak around $\cos\Theta=0.5$ ($\Theta \approx 60°$, characteristic of "hard sphere like" packing) weakens, the peak around $\cos\Theta = -0.33$, $\Theta = 109.5°$, characteristic of tetrahedrally coordinated neighbors, sharpens, and the fraction of bond angles of about 180° decreases considerably, by about 30%. All these alterations indicate consistently that there are more regular (tetrahedral) and less irregular (hard sphere like) angles present in the implanted state than in the evaporated state.

By imposing constraints on bond angles (see Ref. 4)

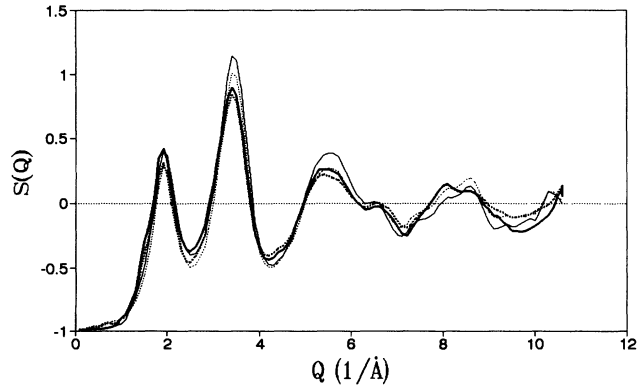

FIG. 4. Measured structure factors of evaporated (heavy solid line) and ion-implanted (solid line) amorphous Ge, and reverse Monte Carlo fits: evaporated (heavy dotted line) and implanted (dotted line).

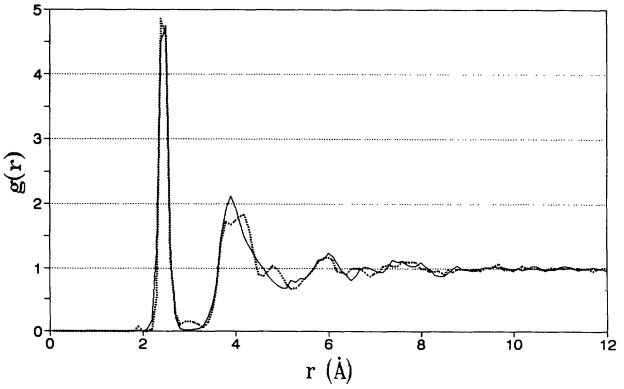

FIG. 5. Pair correlation functions of evaporated (heavy dotted line) and ion-implanted (solid line) amorphous Ge, obtained by reverse Monte Carlo simulation.

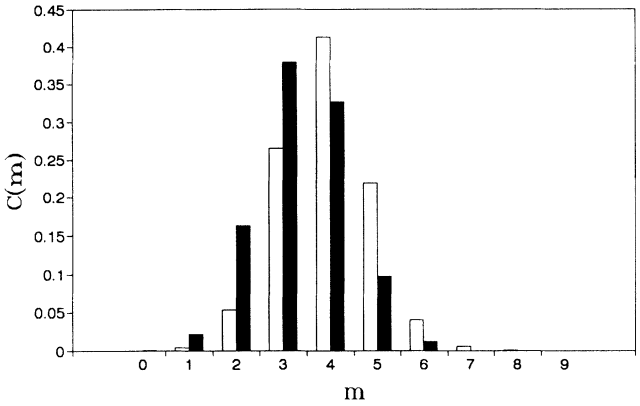

FIG. 6. Distribution of number of first neighbors for evaporated (solid bars) and ion-implanted (open bars) amorphous Ge, obtained from reverse Monte Carlo calculations.

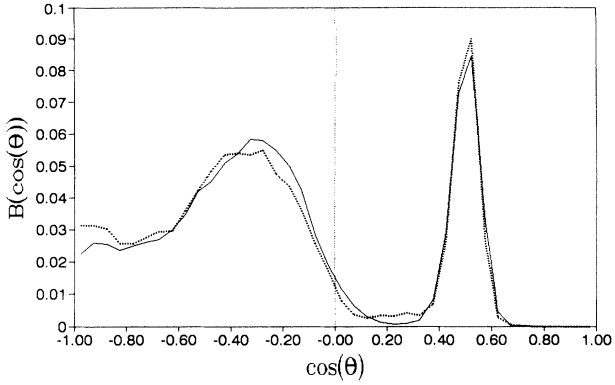

FIG. 7. Cosine distributions of bond angles for evaporated (heavy dotted line) and ion-implanted (solid line) amorphous Ge, obtained from reverse Monte Carlo calculations.

one could have minimized the number of angles far from 109.5°, but this would have disturbed the process of unbiased comparison. Nevertheless, it should be noted that the high percentage of angles of about 60° is probably not a real feature of amorphous Ge. Their presence is an indication of that it is possible to build structural models of a-Ge that contain large amounts of such angles, being consistent with the diffraction data. This is a warning that the diffraction data itself cannot make an unambigous distinction between certain, quite different microscopic structures. The case was entirely similar for amorphous silicon.[4]

Using an unconstrained RMC simulation we can state that the tendency towards forming a more regular tetrahedral (and fourfold coordinated) structure is contained *inherently* in the diffraction data. The RMC simulation therefore served as just a possible tool for extracting this information and making the tendency visible. It is also noted that the small shift and the sharpening around the terahedral peak in Fig. 7 can explain the differences in the second peak of $g(r)$ (see Fig. 5).

According to the above, the effect of implantation is an overall increase of local ordering, if the sample is considered *homogeneous* (i.e., of uniform microscopic density). However, since morphologically the implanted sample is clearly inhomogenous (see Fig. 1), the possibility of the coexistence of—at least—two different states, with two different microscopic densities, cannot be excluded, although the present diffraction data do not imply that. One of these states would be the heavily bombarded lower halves of every layer (shown as almost black, with large white areas in between, on the micrograph of Fig. 1). The other state could be represented by the less affected upper halves of the layers (shown in grey, with small lighter bubbles on the micrograph). In such a case, the average description, given by the RMC simulation, for instance, is not valid for the whole sample. The most exciting feature of the material would then be that in the more dense part atoms should have more than four neighbors (since the average number density of the entire sample is roughly 4). This would mean the formation of a yet unknown new phase of amorphous Ge. Diffraction measurements cannot make an unambigous difference between the two possibilities at this stage. The photoemission data supports the latter suggestion.[15] Even if on the basis of the x-ray data the two possibilities cannot be distinguished, any of the processes would be rather unexpected, since in the case of a-Ge implantation gave rise to an increase of density, along with an improved local ordering. These effects are highly unusual as results of ion bombardment.

This work has been supported by OTKA Grant Nos. F 4320, 2934, and 2963.

[1] R.J. Temkin, W. Paul, and G.A.N. Connel, Adv. Phys. **22**, 581 (1973).
[2] G. Etherington, A.C. Wright, J.T. Wenzel, J.C. Dore, J.H. Clarke, and R.N. Sinclair, J. Non-Cryst. Solids **48**, 265 (1993).
[3] S. Kugler, G. Molnár, G. Petö, L. Rosta, A. Menelle, and R. Bellisent Phys. Rev. B **40**, 8030 (1989).
[4] S. Kugler, L. Pusztai, L. Rosta, R. Bellisent, and P. Chieux, Phys. Rev. B **48**, 7685 (1993).
[5] I. Stich, R. Car, and M. Parinello, Phys. Rev. Lett. **63**, 2240 (1989).
[6] K. Ding and H.C. Andersen, Phys. Rev. B **34**, 6987 (1986).
[7] F. Wooten, K. Winer, and D. Weaire, Phys. Rev. Lett. **54**, 1392 (1985).
[8] G. Petö and J. Kanski, Solid State Commun. **38**, 377 (1981).
[9] R.L. McGreevy and L. Pusztai, Mol. Simulation **1**, 359 (1988).
[10] G. Petö, J. Kanski, and G. Holmen, Appl. Phys. Lett. **55**, 692 (1989).
[11] F. Hajdu, Phys. Status Solidi A **60**, 365 (1980).
[12] Y. Waseda and K. Suzuki, Z. Phys. B **20**, 339 (1975).
[13] O. Gereben and L. Pusztai (unpublished).
[14] G.S. Cargill, J. Appl. Crystllogr. **4**, 277 (1971).
[15] G. Petö, L. Rosta, J. Kanski, A. Barna, A. Menelle, and R. Bellisent, J. Non-Cryst. Solids **125**, 258 (1990).

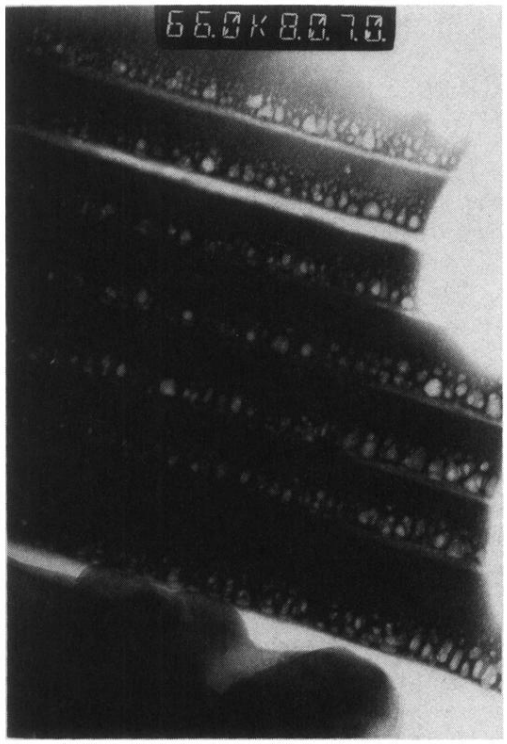

FIG. 1. TEM micrograph of the ion-implanted sample.